Adaptive trajectory tracking control and parameter identification for autonomous underwater vehicles based on contraction theory

Caipeng Ma
Sun Yat-Sen University
Yu Tang
National Autonomous University of Mexico Faculty of Veterinary Medicine and Animal Husbandry: Universidad Nacional Autonoma de Mexico Facultad de Medicina Veterinaria y Zootecnia
Jiaxi Wang
Sun Yat-Sen University
Jiajie Yan
Sun Yat-Sen University
Yuchen Liao
Sun Yat-Sen University
Dapeng Jiang (jiangdp5@mail.sysu.edu.cn)
Sun Yat-Sen University

Research Article

Keywords: Trajectory tracking, AUV, Adaptive control, Parameter identification, Contraction theory

Posted Date: June 9th, 2022

DOI: https://doi.org/10.21203/rs.3.rs-1646233/v1

manuscript No.
(will be inserted by the editor)

Adaptive trajectory tracking control and parameter identification for autonomous underwater vehicles based on contraction theory

Caipeng Ma · Yu Tang · Jiaxi Wang · Jiajie Yan · Yuchen Liao · Dapeng Jiang*

Received: date / Accepted: date

Abstract In this paper, contraction theory is applied to design the trajectory tracking controller for a fully-actuated 6-degree-of-freedom (6-DOF) autonomous underwater vehicle (AUV). First, assuming that all system parameters are known, an ideal controller is given. Then, to deal with the parameter uncertainties, an adaptive controller is proposed. Combined with the adaptive law, the estimated values of the parameters converge to their real values without requiring the persistent excitation (PE) condition to be satisfied, that is, the parameter identification is realized. Exponential convergence of the system is analyzed in the framework of contraction theory. The concepts of partial contraction, virtual system and modular properties reduce the difficulty of system design and analysis. The numerical simulation results show the effectiveness of the proposed method.

Keywords Trajectory tracking · AUV · Adaptive control · Parameter identification · Contraction theory

Caipeng Ma (✉) · Jiaxi Wang (✉) · Jiajie Yan (✉) · Yuchen Liao (✉) · Dapeng Jiang (✉)
School of Marine Engineering and Technology, Sun Yat-Sen University, Zhuhai 519082, China
E-mail: macp3@mail2.sysu.edu.cn
Jiaxi Wang
E-mail: wangjx86@mail2.sysu.edu.cn
Jiajie Yan
E-mail: yanjiajie007@163.com
Yuchen Liao
E-mail: liaoych23@mail2.sysu.edu.cn
Dapeng Jiang
E-mail: jiangdp5@mail.sysu.edu.cn
Yu Tang (✉)
National Autonomous University of Mexico, Mexico City, Mexico
E-mail: tang@unam.mx

1 Introduction

With the development and utilization of the ocean, the influence of AUVs is increasing day by day. At present, AUVs are being used in a variety of disciplines, including oceanographic mapping, environmental monitoring, rescue, scientific research, military and so on [1,2]. Improving the intelligence and efficiency is one of the main objectives of developing AUVs system. Therefore, presentation of advanced controllers is hotspots in the research of AUVs. Many methods for AUVs control have been developed, such as PID control [3,4], backstepping control [5,6], adaptive control [7–10], sliding mode control (SMC) [11–13], model predictive control (MPC) [14,15], active disturbance rejection control (ADRC) [16,17], etc. These methods are used to address the various challenges faced by AUVs control, such as model uncertainties, parameter uncertainties, external disturbances and so on. This paper mainly focuses on the parameter uncertainties.

The uncertainties of model parameters, especially various hydrodynamic coefficients, pose a great challenge to the control of AUVs. How to obtain the hydrodynamic coefficients accurately is also one of current researches of AUVs. From the perspective of hydrodynamics, there are several methods for obtaining hydrodynamic coefficients of marine structures, such as potential theory [18–20], model tests [21,22], Computational Fluid Dynamics (CFD) [23–25] and so on. However, the application of potential theory is limited to simple structures, and thus is incapable of dealing with AUVs with increasingly complex shapes. Model test is considered to be a feasible method, but it is time-consuming and costly. In recent years, with the rapid improvement of computing power, the development of CFD is advancing by leaps and bounds. CFD method is

not limited by the shape of the structure, and the cost is not so expensive compared with the model test, but its effectiveness needs to be further verified. As a result, it is not easy to obtain the hydrodynamic coefficients accurately through hydrodynamics methods.

From the perspective of control, the problem of parameter uncertainties can be solved by a reasonable control algorithm. Adaptive control, as we all know, is one of the control methods that can effectively cope with parameter uncertainties [26]. Therefore, it is widely used in AUVs. In [7], two adaptive algorithms, originally designed for manipulators, were applied to the control of AUVs and a comparative analysis was conducted. [8] and [9] proposed a new adaptive algorithm, in which the dynamic equation of AUVs was linearly parameterized through making reasonable assumptions and selecting appropriate parameters. [27] designed an adaptive controller for an underactuated AUV and 24 parameters need to be estimated on-line. [28] proposed an adaptive trajectory tracking controller for a 4-DOF AUV and the estimated values of unknown parameters remained bounded. In the above literatures, many parameters need to be estimated online, which undoubtedly increases the computational burden To avoid this problem, the controller designed in [29] required only model of gravity and buoyancy and did not need any knowledge of inertia matrix, coriolis and centripetal forces as well as hydrodynamic damping. Therefore, only two parameters need to be updated. [30] proposed a simple adaptive controller based on dynamic surface control technique, with only three parameters to update.

In addition, adaptive control without regression matrix is extensively utilized to circumvent the limitations of model structures. Therefore, state errors and virtual variables are widely used to construct the adaptive algorithm. In [31], the virtual velocities were constructed and their errors were used to stabilize the sway error for an underactuated AUV. In [32], the adaptive fault-tolerant controller was proposed based on the sliding mode variable, which was constructed by state errors and their derivatives. Model parameters are not required for the controller. [10] designed an adaptive algorithm by combining the desired state, state error and their derivatives in a linear manner. A simple 3D trajectory tracking experiment was used to verify its reliability.

Although many of the existing AUVs control methods do not depend on model parameters, accurate model parameters help to understand the properties of the system in order to design a simpler and more efficient controller. However, in the preceding AUVs adaptive control, the estimated values of parameters only remained bounded and did not converge to their real value, therefore the idea of parameter identification via adaptive law was ignored. One of goals of this paper is to make a breakthrough on the subject.

Contraction theory [33] is a powerful tool for nonlinear system analysis and design. Unlike the Lyapunov method, which focuses on the stability of the equilibrium point, contraction theory studies the convergence between the adjacent trajectories of the system [34–36], which gives contraction theory significant advantages in dealing with tracking control problems. Futhermore, the concepts of partial contraction, virtual system and modular properties [37] provide great convenience for the design and analysis of control system. After more than 20 years of development, contraction theory has blossomed and fruited in numerous disciplines [38–44].

In the field of marine vehicles, nonlinear observer based on contraction theory was applied to estimate the position and velocity of AUVs [38,45,46]. [39] proposed a diffusion-based trajectory observer based on contraction theory for underwate vehicle navigation, which was able to reconstruct the trajectory according to the measurements of groy-Doppler and acoustic positioning system in the presence of noises. In [47,48], incremental stability of AUV's system were discussed based on contraction theory, and the speed stabilization controller and trajectory tracking controller were designed using the backstepping method. [49,50] analyzed the tracking problems in a port-Hamiltonian framework rather than the traditional Euler-Lagrangian paradigm, and designed a horizontal trajectory tracking controller for an open-frame underwater unmanned vehilce (UUV) based on contraction theory. In addition, [51,52] designed a globally contracting controller for ship regulation and dynamic positioning using only position measurements. The state observer based on contraction theory was used to estimate the ship's speed and slowly changing environmental disturbance.

Although contraction theory is a powerful tool, its applications in AUVs is still sporadic, and the AUVs model has been greatly simplified in the existing research . In addition, as mentioned above, the parameter identification through adaptive law is often ignored in the adaptive tracking control. This paper focuses on the trajectory tracking control of a 6-DOF AUV, and proposes a new adaptive controller to deal with parameter uncertainty in the framework of contraction theory. And the main contributions are as follows:

(i) Contraction theory is applied to design and analyze the trajectory tracking controller of AUVs. With the help of partial contraction, virtual system and modular properties, the difficulty of control system design and analysis is greatly simplified.

(ii) A new adaptive controller is proposed. Combined with the existing adaptive law, the adaptive controller not only completes the control objective of trajectory tracking, but also realizes the identification of AUV system parameters without satisfying the PE condition, which provides a new method for obtaining the parameters of AUVs system.

The remainder of this work is arranged in the following manner. Section 2 gives the necessary preliminaries on contraction theory. Section 3 establishes a fully-actuated 6-DOF AUV model and its properties useful for the design of controller are also introduced. The ideal controller and adaptive controller are derived in Section 4, and their exponential convergence properties are analyzed with the framework of contraction theory. Section 5 shows the simualtion results and analyses the performance of the controllers. At last, concluding remarks are drawn in section 6.

2 Contraction theory

This section gives a brief introduction to contraction theory. Generally, a system is called contracting if its initial conditions or instantaneous disturbances are forgotten exponentially, that is, all trajectories starting from different initial states eventually converge together exponentially [33].

For a given system:

$$\dot{\mathbf{x}} = \mathbf{f}(\mathbf{x}, t) \tag{1}$$

where $\mathbf{x}$ is the n-dimensional vector corresponding the state fo the system, t is time, and $\mathbf{f}(\mathbf{x}, t)$ is a nonlinear vector field. Assuming $\mathbf{f}(\mathbf{x}, t)$ is continuously differentiable and forward complete.

One of the main features of contraction theory is to use the concept of virtual displacement $\delta\mathbf{x}$ of the state $\mathbf{x}$ which are infinitesimal displacements at fixed time. The so-called virtual dynamics are introduced by calculating the first variation of (1):

$$\delta\dot{\mathbf{x}} = \mathbf{J}(\mathbf{x}, t)\delta\mathbf{x} \tag{2}$$

with $\mathbf{J}(\mathbf{x}, t) = \frac{\partial \mathbf{f}}{\partial t}(\mathbf{x}, t)$ is the Jacobian. In a convex set $\mathscr{X} \subseteq \mathbb{R}^n$ with respect to the metric $\mathcal{M}(\mathbf{x}, t) = \mathbf{P}^T(\mathbf{x}, t)\mathbf{P}(\mathbf{x}, t)$ that is a invertible positive definite matrix, where $\mathbf{P}(\mathbf{x}, t)$ is a $n \times n$ invertible matrix. if there exists some $\lambda > 0$ such that $\forall \mathbf{x} \in \mathscr{X}$ and $t \geq t_0$

$$\dot{\mathcal{M}}(\mathbf{x}, t) + \mathbf{J}^T(\mathbf{x}, t)\mathcal{M}(\mathbf{x}, t) + \mathcal{M}(\mathbf{x}, t)\mathbf{J}(\mathbf{x}, t) \leq -2\lambda\mathcal{M}(\mathbf{x}, t) \tag{3}$$

then, the system (1) is called contracting, $\mathbf{f}(\mathbf{x}, t)$ is called a contracting function. This condition (3) is equivalent to that the symmetric part of the generalized Jacobian $\mathbf{J}_G(x, t) = (\dot{\mathbf{P}} + \mathbf{P}\mathbf{J}(\mathbf{x}, t))\mathbf{P}^{-1}$ is uniformly negative definite, that is, $\mathbf{J}_G(\mathbf{x}, t) \leq -\lambda\mathbf{I}$, $\forall \mathbf{x} \in \mathscr{X}$, where $\mathbf{I}$ is the identity matrix with appropriate dimension. The set $\mathscr{X}$ is called the contraction region and λ is the contraction rate. Moreover, if $\mathscr{X} = \mathbb{R}^n$, the contraction is global. When $\lambda = 0$, the system (1) is said to be semi-contracting.

The squared length between two neighboring trajectories under the metric $\mathcal{M}(\mathbf{x}, t)$ is defined as

$$\mathbf{V} = \delta\mathbf{x}^T\mathcal{M}(\mathbf{x}, t)\delta\mathbf{x}$$

under the condition (3), its time derivative is

$$\begin{aligned}\dot{\mathbf{V}} &= \delta\mathbf{x}^T(\dot{\mathcal{M}}(\mathbf{x}, t) + \mathbf{J}^T(\mathbf{x}, t)\mathcal{M}(\mathbf{x}, t) + \mathcal{M}(\mathbf{x}, t)\mathbf{J}(\mathbf{x}, t))\delta\mathbf{x} \\ &\leq -2\lambda\delta\mathbf{x}^T\mathcal{M}\delta\mathbf{x}\end{aligned}$$

Therefore, the distance between any pair of trajectories under the metric $\mathscr{M}$ converges to zero exponentially.

We now briefly recall the basic principles of an extension of contraction analysis, the so-called partial contraction [37].

Theorem 2.1. **(Partial contraction)** Consider the following auxiliary system called virtual system

$$\dot{\boldsymbol{\xi}} = \bar{\mathbf{f}}(\boldsymbol{\xi}, \mathbf{x}, t) \tag{4}$$

associated with the nonlinear system (1) through $\bar{\mathbf{f}}(\mathbf{x}, \mathbf{x}, t) = \mathbf{f}(\mathbf{x}, t)$. If the virtual system (4) is contracting with respect to $\boldsymbol{\xi}, \forall \boldsymbol{\xi}, \mathbf{x} \in \mathscr{X}, t \geq t_0$. Then, all its particular solutions converge exponentially to each other and in particular $\boldsymbol{\xi}(t) - \mathbf{x}(t) \to 0$ exponentially from any initial condition in $\mathscr{X}$. The original system (1) is said to be partially contracting.

In the tracking control problems, the designer may propose a virtual system which has two particular solutions: the desired trajectory and the actual trajectory. If the virtual system is contracting, then all its particular solutions will converge exponentially to each other, that is, the actual trajectory converges to the desired trajectory exponentially.

For contraction theory, it is automatically preserved through a variety of system combinations, such as parallel, cascade and feedback combinations. This property is beneficial to the modular design of control system. Here, the feedback combination is introduced.

Theorem 2.2. **(Contraction of feedback combination)** Let two systems be connected in feedback form as

$$\begin{aligned}\dot{\mathbf{x}}_1 &= \mathbf{f}_1(\mathbf{x}_1, \mathbf{x}_2, t), \\ \dot{\mathbf{x}}_2 &= \mathbf{f}_2(\mathbf{x}_1, \mathbf{x}_2, t).\end{aligned} \tag{5}$$

Consider the differential dynamics $[\delta\mathbf{x}_1^T \ \delta\mathbf{x}_2^T]^T$, arranged as

$$\frac{d}{dt}\begin{bmatrix}\delta\mathbf{x}_1 \\ \delta\mathbf{x}_2\end{bmatrix} = \begin{bmatrix}\mathbf{F}_1 & \mathbf{F}_{12} \\ \mathbf{F}_{21} & \mathbf{F}_2\end{bmatrix}\begin{bmatrix}\delta\mathbf{x}_1 \\ \delta\mathbf{x}_2\end{bmatrix} \tag{6}$$

If the two subsystems are all contracting, that is, in some region of the state space $\mathbf{F}_1 = \frac{\partial \mathbf{f}_1}{\partial \mathbf{x}_1}$ and $\mathbf{F}_2 = \frac{\partial \mathbf{f}_2}{\partial \mathbf{x}_2}$ are uniformly negative definite, and $\mathbf{F}_{12} = \frac{\partial \mathbf{f}_1}{\partial \mathbf{x}_2} = -\mathbf{F}_{21}^T$, where $\mathbf{F}_{21} = \frac{\partial \mathbf{f}_2}{\partial \mathbf{x}_1}$, then the whole system (5) will be contracting in that region.

A special case of **Theorem 2.2** which allows the x_2-subsystem to be semi-contracting is presented in the following (Chung and Slotine).

Lemma 2.3 **(Semi-contracting)** Consider the nonlinear system

$$\dot{\mathbf{x}} = \begin{bmatrix} \dot{\mathbf{x}}_1 \\ \dot{\mathbf{x}}_2 \end{bmatrix} = \begin{bmatrix} \mathbf{f}_1(\mathbf{x}_1, \mathbf{x}_2, t) \\ \mathbf{f}_2(\mathbf{x}_1, \mathbf{x}_2, t) \end{bmatrix} \tag{7}$$

Let symmetrical part of the Jacobian matrix be given by

$$\mathbf{J}_s = \begin{bmatrix} \mathbf{F}_{1s}(\mathbf{x}_1, \mathbf{x}_2, t) & \mathbf{0} \\ \mathbf{0} & \mathbf{F}_{2s}(\mathbf{x}_1, \mathbf{x}_2, t) \end{bmatrix} \tag{8}$$

Assume that

$$\mathbf{F}_{1s}(\mathbf{x}_1, \mathbf{x}_2, t) \leq -\lambda_1 \mathbf{I}, \ \lambda_1 > 0, \tag{9}$$

$$\mathbf{F}_{2s}(\mathbf{x}_1, \mathbf{x}_2, t) \leq -\lambda_2 \mathbf{I}, \ \lambda_2 \geq 0. \tag{10}$$

Then
(1) If $\lambda_2 > 0$, the system (7) is contracting and all its trajectories converge exponentially to each other.
(2) If $\lambda_2 \geq 0$, the system (7) is semi-contracting and the trajectories of $\mathbf{x}_1$ converge asymptotically to each other while $\delta \mathbf{x}_2$ remains bounded.

3 AUV modeling

In this section, a fully-actuated 6-DOF AUV model is established. In general, it is convenient to use two coordinate systems to describe the motion of AUVs, one is Earth-fixed frame, the other is the body-fixed frame, as shown in Fig. 1.

Then, the nonlinear dynamics of the AUVs is given on the basis of the two coordinates. The quantities are defined according to [53], and the motion of AUVs in 3D space can be described by the following vectors:

$$\boldsymbol{\eta} = [\boldsymbol{\eta}_1^T \ \boldsymbol{\eta}_2^T]^T = [x \ y \ z \ \phi \ \theta \ \psi]^T$$
$$\mathbf{v} = [\mathbf{v}_1^T \ \mathbf{v}_2^T]^T = [u \ v \ w \ p \ q \ r]^T$$

where $\boldsymbol{\eta}_1 = [x \ y \ z]^T \in \mathbb{R}^3$ represents the AUVs position and $\boldsymbol{\eta}_2 = [\phi \ \theta \ \psi]^T \in \mathbb{R}^3$ represents the attitude parameterized in the Euler angle, both of them are expressed in the Earth-fixed frame. The velocity $\mathbf{v} = [\mathbf{v}_1^T \ \mathbf{v}_2^T]^T$ is composed of the linear velocity $\mathbf{v}_1 = [u \ v \ w]^T \in \mathbb{R}^3$ and the angular velocity $\mathbf{v}_2 = [p \ q \ r]^T \in \mathbb{R}^3$ of the AUVs expressed in the body-fixed frame.

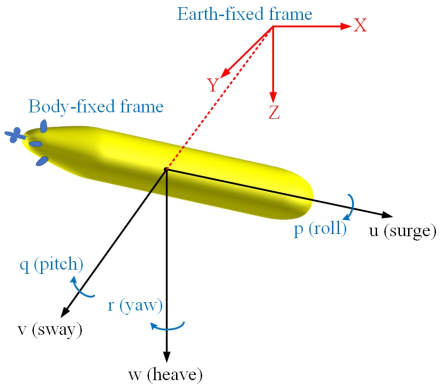

Fig. 1 Earth-fixed frame and body-fixed frame for AUV

Based on the above definitions and descriptions, the kinematic and dynamic equations for a fully-actuated AUV can be expressed as [54]:

$$\begin{cases} \dot{\boldsymbol{\eta}} = \mathbf{J}(\boldsymbol{\eta}_2)\mathbf{v} & (11) \\ \mathbf{M}\dot{\mathbf{v}} = -\mathbf{C}(\mathbf{v})\mathbf{v} - \mathbf{D}(\mathbf{v})\mathbf{v} - \mathbf{G}(\boldsymbol{\eta}_2) - \boldsymbol{\tau}_c + \boldsymbol{\tau} & (12) \end{cases}$$

where $\boldsymbol{\tau} = [\tau_1 \ \tau_2 \ \tau_3 \ \tau_4 \ \tau_5 \ \tau_6]^T \in \mathbb{R}^6$ is the vector of control inputs, $\boldsymbol{\tau}_c \in \mathbb{R}^6$ is the external disturbances caused by ocean current expressed in the body-fixed frame.

The transformation matrix $\mathbf{J}(\boldsymbol{\eta}_2)$ in the kinematic equation (11) is given as

$$\mathbf{J}(\boldsymbol{\eta}_2) = \begin{bmatrix} \mathbf{R}(\boldsymbol{\eta}_2) & \mathbf{0}_{3\times3} \\ \mathbf{0}_{3\times3} & \mathbf{T}(\boldsymbol{\eta}_2) \end{bmatrix} \tag{13}$$

$$\mathbf{R}(\boldsymbol{\eta}_2) = \begin{bmatrix} c\psi c\theta & -s\psi c\phi + c\psi s\theta s\phi & s\psi s\phi + c\psi c\phi s\theta \\ s\psi c\theta & c\psi c\phi + s\phi s\theta s\psi & -c\psi s\phi + s\theta s\psi c\phi \\ -s\theta & c\theta s\phi & c\theta c\phi \end{bmatrix} \tag{14}$$

$$\mathbf{T}(\boldsymbol{\eta}_2) = \begin{bmatrix} 1 & s\phi t\theta & c\phi t\theta \\ 0 & c\phi & -s\phi \\ 0 & s\phi/c\theta & c\phi/c\theta \end{bmatrix} \tag{15}$$

where $c(\cdot) = cos(\cdot), s(\cdot) = sin(\cdot)$ and $t(\cdot) = tan(\cdot)$.

In the dynamic equation (12), $\mathbf{M} \in \mathbb{R}^{6\times6}$ represents the inertial matrix, including the added mass, $\mathbf{C}(\mathbf{v}) \in \mathbb{R}^{6\times6}$ is the coriolis and centripetal term includes the effect of added mass, $\mathbf{D}(\mathbf{v}) \in \mathbb{R}^{6\times6}$ is the friction and hydrodynamic damping matrix.

$$\mathbf{M} = diag(m_{11}, \ m_{22}, \ m_{33}, \ m_{44}, \ m_{55}, \ m_{66}) \tag{16}$$

where $m_{11} = m - X_{\dot{u}}, m_{22} = m - Y_{\dot{v}}, m_{33} = m - Z_{\dot{w}}, m_{44} = I_x - K_{\dot{p}}, m_{55} = I_y - M_{\dot{q}}, m_{66} = I_z - N_{\dot{r}}$. m is the mass of the AUV, I_x, I_y and I_z are the moments of inertia about the roll, pitch and yaw rotation,

respectively. $X_{\dot{u}}, Y_{\dot{v}}, Z_{\dot{w}}, K_{\dot{p}}, M_{\dot{q}}, N_{\dot{r}}$ are the hydrodynamic coefficients relative to added mass.

$$\mathbf{C}(\mathbf{v}) = \begin{bmatrix} \mathbf{0}_{3\times3} & \mathbf{C}_{12} \\ \mathbf{C}_{21} & \mathbf{C}_{22} \end{bmatrix} \tag{17}$$

$$\mathbf{C}_{12} = \mathbf{C}_{21} = \begin{bmatrix} 0 & m_{33}w & -m_{22}v \\ -m_{33}w & 0 & m_{11}u \\ m_{22}v & -m_{11}u & 0 \end{bmatrix}$$

$$\mathbf{C}_{22} = \begin{bmatrix} 0 & m_{66}r & -m_{55}q \\ -m_{66}r & 0 & m_{44}p \\ m_{55}q & -m_{44}p & 0 \end{bmatrix}$$

$$\mathbf{D}(\mathbf{v}) = diag(d_{11}|u|, d_{22}|v|, d_{33}|w|, d_{44}|p|, d_{55}|q|, d_{66}|r|) \tag{18}$$

$d_{11} = -X_{|u|u}, d_{22} = -Y_{|v|v}, d_{33} = -Z_{|w|w}, d_{44} = -K_{|p|p}$, $d_{55} = -M_{|q|q}, d_{66} = -N_{|r|r}$ are damping coefficients.

$\mathbf{G}(\boldsymbol{\eta}_2) \in \mathbb{R}^6$ is the gravitational and buoyant (restoring) generalized forces/torques:

$$\mathbf{G}(\boldsymbol{\eta}_2) = \begin{bmatrix} (W-B)s\theta \\ -(W-B)c\theta s\phi \\ -(W-B)c\theta c\phi \\ -(y_gW - y_bB)c\theta c\phi + (z_gW - z_bB)c\theta s\phi \\ (z_gW - z_bB)s\theta + (x_gW - x_bB)c\theta c\phi \\ -(x_gW - x_bB)c\theta s\phi - (y_gW - y_bB)s\theta \end{bmatrix} \tag{19}$$

$W = mg$ is the vehicle's weight, g is the gravity acceleration. B is the buoyancy force. $\mathbf{r}_g = [x_g \ y_g \ z_g]^T$ and $\mathbf{r}_b = [x_b \ y_b \ z_b]^T$ denote the center of gravity and the center of buoyancy in the body-fixed frame, respectively.

The disturbances $\boldsymbol{\tau}_c$ caused by the ocean current expressed in the Earth-fixed frame is a constant vector under the assumption that the ocean current is constant and irrational [9]:

$$\boldsymbol{\tau}_c = \boldsymbol{\Phi}_c(\boldsymbol{\eta}_2)\boldsymbol{\Theta}_c \tag{20}$$

where $\boldsymbol{\Theta}_c = [\tau_{c1} \ \tau_{c2} \ \tau_{c3} \ \tau_{c4} \ \tau_{c5} \ \tau_{c6}]^T \in \mathbb{R}^6$, and

$$\boldsymbol{\Phi}_c(\boldsymbol{\eta}_2) = \begin{bmatrix} \mathbf{R}^T(\boldsymbol{\eta}_2) & \mathbf{0}_{3\times3} \\ \mathbf{0}_{3\times3} & \mathbf{R}^T(\boldsymbol{\eta}_2) \end{bmatrix} \tag{21}$$

Remark 3.1. The matrices $\mathbf{M}$, $\mathbf{C}(\mathbf{v})$ and $\mathbf{D}(\mathbf{v})$ have the following properties:
(1) The inertial matrix $\mathbf{M} \in \mathbb{R}^{6\times6}$ satisfies $\mathbf{M} = \mathbf{M}^T > 0$.
(2) $\mathbf{C}(\mathbf{v}) \in \mathbb{R}^{6\times6}$ is a skew-symmetric matrix, i.e., $\mathbf{C}(\mathbf{v}) = -\mathbf{C}^T(\mathbf{v}), \ \forall \mathbf{v} \in \mathbb{R}^6$.
(3) $\mathbf{D}(\mathbf{v}) \in \mathbb{R}^{6\times6}$ satisfies $\mathbf{D}(\mathbf{v}) = \mathbf{D}^T(\mathbf{v}) \geq 0, \ \forall \mathbf{v} \in \mathbb{R}^6$.

Assumption 3.1. The transformation matrix $\mathbf{J}(\boldsymbol{\eta}_2)$ is invertible, i.e., $|\theta| \neq \pm\frac{\pi}{2}$.

Remark 3.2. $\mathbf{T}(\boldsymbol{\eta}_2)$ is singular if $|\theta| = \pm\frac{\pi}{2}$. Therefore, this phenomenon needs to be avoided. Fortunately, in practical application, this can be done. First, due to metacentric restoring forces, AUVs are unlikely to enter the regions of $\theta = \pm\frac{\pi}{2}$. Then, the desired trajectory for θ can be chosen that is sufficiently far from the singularity point.

Assumption 3.3. When the AUV travels in a uniform and irrational ocean current at low speed, the hydrodynamic coefficients remain unchanged or change very slowly, resulting in $\dot{\mathbf{M}} = 0$. In addition, the external disturbances vector $\boldsymbol{\Theta}_c$ caused by ocean current is constant expressed in the Earth-fixed frame,

According to ***Assumption 3.3***, by selecting appropriate parameters, the dynamic equation (12) can be linearly parameterized as:

$$\boldsymbol{\tau} = \boldsymbol{\Phi}(\boldsymbol{\eta}_2, \mathbf{v}, \dot{\mathbf{v}})\boldsymbol{\Theta} \tag{22}$$

which will be used in the design of adaptive controller. Where, $\boldsymbol{\Theta} = [\boldsymbol{\Theta}_1^T \ \boldsymbol{\Theta}_2^T \ \boldsymbol{\Theta}_c^T]^T$ is the system parameters. $\boldsymbol{\Theta}_1 = [m_{11} \ m_{22} \ m_{33} \ m_{44} \ m_{55} \ m_{66} \ d_{11} \ d_{22} \ d_{33} \ d_{44} \ d_{55} \ d_{66}]^T$, $\boldsymbol{\Theta}_2 = [-(W-B) \ (x_GW - x_BB) \ (y_GW - y_BB) \ (z_GW - z_BB)]^T$. $\boldsymbol{\Phi}(\boldsymbol{\eta}_2, \mathbf{v}, \dot{\mathbf{v}}) = [\boldsymbol{\Phi}_1 \ \boldsymbol{\Phi}_2 \ \boldsymbol{\Phi}_3 \ \boldsymbol{\Phi}_c(\boldsymbol{\eta}_2)]$ is the regressor matrix.

$$\boldsymbol{\Phi}_1 = \begin{bmatrix} \dot{u} & -vr & wq & 0 & 0 & 0 \\ ur & \dot{v} & -wp & 0 & 0 & 0 \\ -uq & vp & \dot{w} & 0 & 0 & 0 \\ 0 & -vw & wv & \dot{p} & -qr & rq \\ uw & 0 & -wu & pr & \dot{q} & -rp \\ -uv & vu & 0 & -pq & qp & \dot{r} \end{bmatrix} \tag{23}$$

$$\boldsymbol{\Phi}_2 = \begin{bmatrix} |u|u & 0 & 0 & 0 & 0 & 0 \\ 0 & |v|v & 0 & 0 & 0 & 0 \\ 0 & 0 & |w|w & 0 & 0 & 0 \\ 0 & 0 & 0 & |p|p & 0 & 0 \\ 0 & 0 & 0 & 0 & |q|q & 0 \\ 0 & 0 & 0 & 0 & 0 & |r|r \end{bmatrix} \tag{24}$$

$$\boldsymbol{\Phi}_3 = \begin{bmatrix} -s_\theta & 0 & 0 & 0 \\ c_\theta s_\phi & 0 & 0 & 0 \\ c_\theta c_\phi & 0 & 0 & 0 \\ 0 & 0 & -c_\theta c_\phi & c_\theta s_\phi \\ 0 & c_\theta c_\phi & 0 & s_\theta \\ 0 & -c_\theta s_\phi & -s_\theta & 0 \end{bmatrix} \tag{25}$$

Notice that the regression matrix $\boldsymbol{\Phi}(\boldsymbol{\eta}_2, \mathbf{v}, \dot{\mathbf{v}})$ depends on the attitude $\boldsymbol{\eta}_2$, the velocity $\mathbf{v}$ and the acceleration $\dot{\mathbf{v}}$. For AUVs, the attitude can be obtained by the inertial navigation system (INS) and the velocity may be measured by Doppler velocity log (DVL). Although the acceleration is available through some equipments, it is very noisy and contains bias, especaily for low cost sensors . In order to eliminate the dependence on

acceleration, a filtered version of regression matrix is defined. Let

$$\boldsymbol{\tau}_f = f(s)\boldsymbol{\tau} \tag{26}$$

be the filtered version of $\boldsymbol{\tau}$, where $f(s) = \frac{\lambda_f}{s+\lambda_f}$ is a linear stable and strictly proper filter, $\lambda_f > 0$ is the filter gain. Therefore

$$\boldsymbol{\tau}_f = \boldsymbol{\Phi}_f(\boldsymbol{\eta}_2, \mathbf{v})\boldsymbol{\Theta} \tag{27}$$

with $\boldsymbol{\Phi}_f(\boldsymbol{\eta}_2, \mathbf{v})$ is the filtered regressor matrix.

4 Controller Design

This section presents the design process of two controllers. First, an ideal state feedback controller assuming the knowledge of parameter vector $\boldsymbol{\Theta}$ in (22) is devised. Then, the parameter vector is substituted in a certainty equivalence fashion by its estimated value to obtain an adaptive controller. Their exponential convergence properties are proved by contraction theory.

Give a desired trajectory $\boldsymbol{\eta}_d(t) = [x_d(t)\ y_d(t)\ z_d(t)\ \phi_d(t)\ \theta_d(t)\ \psi_d(t)]^T$, each term is uniformly continuous and bounded, expressed at the Earth-fixed frame. The control objective is to drive $\boldsymbol{\eta}(t) \to \boldsymbol{\eta}_d(t)$ exponentially.

4.1 Ideal controller design

First, an ideal state feedback controller is devised under the assumption that all system parameters are known. Therefore, an ideal controller is proposed as:

$$\begin{aligned}\boldsymbol{\tau} = {} & \mathbf{M}\dot{\mathbf{v}}_r + \mathbf{C}(\mathbf{v})\mathbf{v}_r + \mathbf{D}(\mathbf{v})\mathbf{v}_r + \mathbf{G}(\boldsymbol{\eta}_2) + \boldsymbol{\tau}_c \\ & - \mathbf{J}^T(\boldsymbol{\eta}_2)(\boldsymbol{\eta} - \boldsymbol{\eta}_d) - \mathbf{K}_D(\mathbf{v} - \mathbf{v}_r)\end{aligned} \tag{28}$$

$$\mathbf{v}_r = \mathbf{J}^{-1}(\boldsymbol{\eta}_2)\dot{\boldsymbol{\eta}}_r,\ \dot{\boldsymbol{\eta}}_r = \dot{\boldsymbol{\eta}}_d - \mathbf{K}_p(\boldsymbol{\eta} - \boldsymbol{\eta}_d) \tag{29}$$

$$\dot{\mathbf{v}}_r = \mathbf{J}^{-1}(\boldsymbol{\eta}_2)(\ddot{\boldsymbol{\eta}}_r - \dot{\mathbf{J}}(\boldsymbol{\eta}_2)\mathbf{v}_r) \tag{30}$$

where $\mathbf{K}_D = \mathbf{K}_D^T > 0$ and $\mathbf{K}_p = \mathbf{K}_p^T > 0$ are control gains, $\mathbf{v}_r$ is the reference velocity, $\dot{\mathbf{J}}^{-1} = -\mathbf{J}^{-1}\dot{\mathbf{J}}\mathbf{J}^{-1}$ was used in computing $\dot{\mathbf{v}}_r$.

Theorem 4.1. Accoding to the definitions of $\mathbf{K}_D$ and $\mathbf{K}_p$, the controller defined by (28)-(30) drives $[\boldsymbol{\eta}^T\ \mathbf{v}^T]^T$ converge to $[\boldsymbol{\eta}_d^T\ \mathbf{v}_r^T]^T$ exponentially from any initial conditions.

Proof: the control law (28)-(30) may be rearranged as:

$$\begin{cases}\mathbf{M}\dot{\mathbf{v}}_r = -\mathbf{C}(\mathbf{v})\mathbf{v}_r - \mathbf{D}(\mathbf{v})\mathbf{v}_r - \mathbf{G}(\boldsymbol{\eta}_2) - \boldsymbol{\tau}_c + \boldsymbol{\tau} \\ \qquad\quad +\mathbf{K}_D(\mathbf{v} - \mathbf{v}_r) + \mathbf{J}^T(\boldsymbol{\eta}_2)(\boldsymbol{\eta} - \boldsymbol{\eta}_d) \\ \dot{\boldsymbol{\eta}}_d = \mathbf{J}(\boldsymbol{\eta}_2)\mathbf{v}_r + \mathbf{K}_p(\boldsymbol{\eta} - \boldsymbol{\eta}_d)\end{cases} \tag{31}$$

The controller (31) and AUV system (11-12) suggest the virtual system:

$$\begin{cases}\mathbf{M}\dot{\boldsymbol{\xi}}_1 = -\mathbf{C}(\mathbf{v})\boldsymbol{\xi}_1 - \mathbf{D}(\mathbf{v})\boldsymbol{\xi}_1 - \mathbf{G}(\boldsymbol{\eta}_2) - \boldsymbol{\tau}_c + \boldsymbol{\tau} \\ \qquad\quad +\mathbf{K}_D(\mathbf{v} - \boldsymbol{\xi}_1) + \mathbf{J}^T(\boldsymbol{\eta}_2)(\boldsymbol{\eta} - \boldsymbol{\xi}_2) \\ \dot{\boldsymbol{\xi}}_2 = \mathbf{J}(\boldsymbol{\eta}_2)\boldsymbol{\xi}_1 + \mathbf{K}_p(\boldsymbol{\eta} - \boldsymbol{\xi}_2)\end{cases} \tag{32}$$

Obviously, the virtual system $\boldsymbol{\xi} = [\boldsymbol{\xi}_1^T\ \boldsymbol{\xi}_2^T]^T$ has two particular solutions for any given initial conditions: $\boldsymbol{\xi} = [\boldsymbol{\eta}^T\ \mathbf{v}^T]^T$ and $\boldsymbol{\xi} = [\boldsymbol{\eta}_d^T\ \mathbf{v}_r^T]^T$ which correspond to the AUV system (11-12) and controller system (31), respectively. The differential dynamics of the virtual system is given by:

$$\mathcal{M}_1\delta\dot{\boldsymbol{\xi}} = \mathbf{J}_1\delta\boldsymbol{\xi} \tag{33}$$

where $\delta\boldsymbol{\xi} = [\delta\boldsymbol{\xi}_1^T\ \delta\boldsymbol{\xi}_2^T]^T$, $\mathcal{M}_1 = diag(\mathbf{I}_6, \mathbf{M})$ is the metric, $\mathbf{J}_1$ is the Jacobian,

$$\mathbf{J}_1 = \begin{bmatrix}-\mathbf{K}_p & \mathbf{J}(\boldsymbol{\eta}_2) \\ -\mathbf{J}^T(\boldsymbol{\eta}_2) & -(\mathbf{C}(\mathbf{v}) + \mathbf{D}(\mathbf{v}) + \mathbf{K}_D)\end{bmatrix} \tag{34}$$

Take $\mathcal{M}_1$ as the metric, the squared distance between any two trajectories under the metric is defined as $V_1 = \delta\boldsymbol{\xi}^T\mathcal{M}_1\delta\boldsymbol{\xi}$, and its time derivative is

$$\dot{V}_1 = 2\delta\boldsymbol{\xi}^T\mathcal{M}_1\delta\dot{\boldsymbol{\xi}} = 2\delta\boldsymbol{\xi}^T\mathbf{J}_{1,s}\delta\boldsymbol{\xi} \tag{35}$$

where $\mathbf{J}_{1,s} = (\mathbf{J}_1 + \mathbf{J}_1^T)/2$ is the symmetric part of $\mathbf{J}_1$:

$$\begin{aligned}\mathbf{J}_{1,s} &= -\begin{bmatrix}\mathbf{K}_p & \mathbf{0}_{6\times6} \\ \mathbf{0}_{6\times6} & (\mathbf{D}(\mathbf{v}) + \mathbf{K}_D)\end{bmatrix} \\ &\leq -\begin{bmatrix}\mathbf{K}_p & \mathbf{0}_{6\times6} \\ \mathbf{0}_{6\times6} & \mathbf{K}_D\end{bmatrix} < 0\end{aligned} \tag{36}$$

Here, the properties given in ***Remark 3.1*** and the definitions of $\mathbf{K}_P, \mathbf{K}_D$ are used. Therefore, $\dot{V}_1 \leq -2\lambda_1 V_1$, the virtual system is contracting under the metric $\mathcal{M}_1$ with the contraction rate $\lambda_1 = \frac{min\{\lambda_{min}(\mathbf{K}_D), \lambda_{min}(\mathbf{K}_p)\}}{\lambda_{max}(\mathcal{M}_1)}$, $\lambda_{max}(\cdot)$ and $\lambda_{min}(\cdot)$ denote the maximum and minimum eigenvalue of a matrix, respectively. As a consequence, $[\boldsymbol{\eta}^T\ \mathbf{v}^T]^T \to [\boldsymbol{\eta}_d^T\ \mathbf{v}_r^T]^T$ exponentially from any initial conditions.

4.2 Adaptive controller design

As mentioned above, it is difficult to accurately obtain various hydrodynamic coefficients of AUVs, so adaptive control is needed to deal with parameter uncertainties. In this subsection, the framework of contraction theory is used to design an adaptive controller. Towards this end, the ideal controller (28) can be rewritten according to (22), as

$$\boldsymbol{\tau} = \boldsymbol{\Phi}(\boldsymbol{\eta}_2, \mathbf{v}, \mathbf{v}_r, \dot{\mathbf{v}}_r)\boldsymbol{\Theta} - \mathbf{J}^T(\boldsymbol{\eta}_2)(\boldsymbol{\eta} - \boldsymbol{\eta}_d) - \mathbf{K}_D(\mathbf{v} - \mathbf{v}_r) \tag{37}$$

Applying the principle of certainty equivalence, the adaptive controller can be obtained by replacing the system parameter $\boldsymbol{\Theta}$ in the ideal controller with its estimated value $\hat{\boldsymbol{\Theta}}(t)$:

$$\boldsymbol{\tau} = \boldsymbol{\Phi}(\boldsymbol{\eta}_2, \mathbf{v}, \mathbf{v}_r, \dot{\mathbf{v}}_r)\hat{\boldsymbol{\Theta}}(t) - \mathbf{J}^T(\boldsymbol{\eta}_2)(\boldsymbol{\eta} - \boldsymbol{\eta}_d) - \mathbf{K}_D(\mathbf{v} - \mathbf{v}_r)$$

(38)

The parameter vector is updated by the adaptive law in [55]:

$$\begin{cases} \dot{\hat{\boldsymbol{\Theta}}}(t) = -\boldsymbol{\Gamma}(\boldsymbol{\Phi}^T(\boldsymbol{\eta}_2, \mathbf{v}, \mathbf{v}_r, \dot{\mathbf{v}}_r)(\mathbf{v} - \mathbf{v}_r) + K_{\boldsymbol{\Theta}}\boldsymbol{\beta}(t)) & (39) \\ \dot{\boldsymbol{\beta}}(t) = -(\frac{1}{\varepsilon_m}\mathbf{I} + \boldsymbol{\Gamma}\mathbf{K}_{\boldsymbol{\Theta}}\mathbf{Z}(t))\boldsymbol{\beta}(t) + \frac{1}{\varepsilon_m}\boldsymbol{\Phi}_f^T(\boldsymbol{\eta}_2, \mathbf{v})\boldsymbol{\varepsilon} \\ \qquad -\boldsymbol{\Gamma}\boldsymbol{Z}(t)\boldsymbol{\Phi}^T(\boldsymbol{\eta}_2, \mathbf{v}, \mathbf{v}_r, \dot{\mathbf{v}}_r)(\mathbf{v} - \mathbf{v}_r) & (40) \\ \dot{\mathbf{Z}}(t) = \frac{1}{\varepsilon_m}(\boldsymbol{\Phi}_f^T(\boldsymbol{\eta}_2, \mathbf{v})\boldsymbol{\Phi}_f(\boldsymbol{\eta}_2, \mathbf{v}) - \boldsymbol{Z}(t)) & (41) \end{cases}$$

The initial values of $\boldsymbol{\beta}$ and $\mathbf{Z}$ are both $\mathbf{0}$. As for the initial value of $\hat{\boldsymbol{\Theta}}(t)$, if there are some prior knowledge of system parameters, a reasonable initial guess may be chosen. $\boldsymbol{\varepsilon} = \hat{\boldsymbol{\tau}}_f - \boldsymbol{\tau}_f$, where $\hat{\boldsymbol{\tau}}_f = \boldsymbol{\Phi}_f(\boldsymbol{\eta}_2, \mathbf{v})\hat{\boldsymbol{\Theta}}(t)$ and $\boldsymbol{\Phi}_f(\boldsymbol{\eta}_2, \mathbf{v})$ has been given in (27). $\boldsymbol{\Gamma} > 0$ and $\mathbf{K}_{\boldsymbol{\Theta}} > 0$ are diagonal gain matrices, $\varepsilon_m \geq 0$ represents the memory of the adaptive law.

Definition 4.1. (Sufficient Excitation): The uniformly bounded regressor $\boldsymbol{\Phi}_f(t) = \boldsymbol{\Phi}_f(\boldsymbol{\eta}_2(t), \mathbf{v}(t)) \in R^{6\times n_{\boldsymbol{\Theta}}}$ is said to be sufficiently exciting if there exist $\lambda_{\mathbf{Z}} > 0$ and $T > 0$, such that

$$\int_0^t e^{-(t-\tau)/\varepsilon_m}\boldsymbol{\Phi}_f^T(\tau)\boldsymbol{\Phi}_f(\tau)d\tau \geq \lambda_{\mathbf{Z}}\mathbf{I}, \forall t \geq T \tag{42}$$

Theorem 4.2. Consider the adaptive controller (38) with the adaptive law (39-41). According to (41) and the initial condition $\mathbf{Z}(0) = \mathbf{0}$, $\mathbf{Z}(t)$ can be expressed as:

$$\boldsymbol{Z}(t) = \frac{1}{\varepsilon_m}\int_0^t e^{-(t-\tau)/\varepsilon_m}\boldsymbol{\Phi}_f^T(\tau)\boldsymbol{\Phi}_f(\tau)d\tau \geq \lambda_{\mathbf{Z}}\mathbf{I}, \forall t \geq T > 0 \tag{43}$$

Then from any initial conditions,
(1) if $\lambda_{\mathbf{Z}} > 0$, i.e., $\boldsymbol{\Phi}_f(t)$ is sufficiently exciting, then $[\boldsymbol{\eta}^T(t)\ \mathbf{v}^T(t)\ \hat{\boldsymbol{\Theta}}^T(t)]^T \to [\boldsymbol{\eta}_d^T(t)\ \mathbf{v}_r^T(t)\ \boldsymbol{\Theta}^T]^T$ exponentially;
(2) if $\lambda_{\mathbf{Z}} \geq 0$, then $[\boldsymbol{\eta}^T(t)\ \mathbf{v}^T(t)]^T \to [\boldsymbol{\eta}_d^T(t)\ \mathbf{v}_r^T(t)]^T$ asymptotically, and $\hat{\boldsymbol{\Theta}}(t)$ is bounded for all $t \geq 0$.
Proof: Combining with (29), (37) and (38), the adaptive controller may be rearranged as:

$$\begin{cases} \dot{\boldsymbol{\eta}}_d = \mathbf{J}(\boldsymbol{\eta}_2)\mathbf{v}_r + \mathbf{K}_p(\boldsymbol{\eta} - \boldsymbol{\eta}_d) \\ \mathbf{M}\dot{\mathbf{v}}_r = -\mathbf{C}(\mathbf{v})\mathbf{v}_r - \mathbf{D}(\mathbf{v})\mathbf{v}_r - \mathbf{G}(\boldsymbol{\eta}_2) - \boldsymbol{\tau}_c + \mathbf{K}_D(\mathbf{v} - \mathbf{v}_r) \\ \qquad \mathbf{J}^T(\boldsymbol{\eta}_2)(\boldsymbol{\eta} - \boldsymbol{\eta}_d) - \boldsymbol{\Phi}(\boldsymbol{\eta}_2, \mathbf{v}, \mathbf{v}_r, \dot{\mathbf{v}}_r)(\hat{\boldsymbol{\Theta}} - \boldsymbol{\Theta}) + \boldsymbol{\tau} \end{cases} \tag{44}$$

It has been proven that $\boldsymbol{\beta}(t) = \boldsymbol{Z}(t)(\hat{\boldsymbol{\Theta}} - \boldsymbol{\Theta})$, the rigorous proof can be found in [55]. Therefore, the adaptive law (39) may be rewritten as

$$\boldsymbol{\Gamma}^{-1}\dot{\hat{\boldsymbol{\Theta}}} = -\boldsymbol{\Phi}^T(\boldsymbol{\eta}_2, \mathbf{v}, \mathbf{v}_r, \dot{\mathbf{v}}_r)(\mathbf{v} - \mathbf{v}_r) - K_{\boldsymbol{\Theta}}\boldsymbol{Z}(t)(\hat{\boldsymbol{\Theta}} - \boldsymbol{\Theta}) \tag{45}$$

Then, according to (44-45), the virtual system is obviously obtained:

$$\begin{cases} \dot{\boldsymbol{\xi}}_1 = J(\boldsymbol{\eta}_2)\boldsymbol{\xi}_2 + \mathbf{K}_p(\boldsymbol{\eta} - \boldsymbol{\xi}_1) \\ \mathbf{M}\dot{\boldsymbol{\xi}}_2 = -\mathbf{C}(\mathbf{v})\boldsymbol{\xi}_2 - \mathbf{D}(\mathbf{v})\boldsymbol{\xi}_2 - \mathbf{G}(\boldsymbol{\eta}_2) - \boldsymbol{\tau}_c + \mathbf{K}_D(\mathbf{v} - \boldsymbol{\xi}_2) \\ \qquad +\boldsymbol{\tau} + \mathbf{J}^T(\boldsymbol{\eta}_2)(\boldsymbol{\eta} - \boldsymbol{\xi}_1) - \boldsymbol{\Phi}(\boldsymbol{\eta}_2, \mathbf{v}, \mathbf{v}_r, \dot{\mathbf{v}}_r)(\boldsymbol{\xi}_3 - \boldsymbol{\Theta}) \\ \boldsymbol{\Gamma}^{-1}\dot{\boldsymbol{\xi}}_3 = -\boldsymbol{\Phi}^T(\boldsymbol{\eta}_2, \mathbf{v}, \mathbf{v}_r, \dot{\mathbf{v}}_r)(\mathbf{v} - \boldsymbol{\xi}_2) - \mathbf{K}_{\boldsymbol{\Theta}}\boldsymbol{Z}(t)(\boldsymbol{\xi}_3 - \boldsymbol{\Theta}) \end{cases} \tag{46}$$

Notice that $\boldsymbol{\xi} = [\boldsymbol{\xi}_1^T\ \boldsymbol{\xi}_2^T\ \boldsymbol{\xi}_3^T]^T$ in the virtual system (46) has two particular solutions: $\boldsymbol{\xi}_1 = [\boldsymbol{\eta}^T\ \mathbf{v}^T\ \boldsymbol{\Theta}^T]^T$ and $\boldsymbol{\xi}_2 = [\boldsymbol{\eta}_d^T\ \mathbf{v}_r^T\ \hat{\boldsymbol{\Theta}}^T]^T$, corresponding to AUVs system (11-12) and the adaptive controller (44-45), respectively. It should be noted that when $\boldsymbol{\xi} = \boldsymbol{\xi}_1$, the first two equations of the virtual system (46) correspond to (11) and (12) respectively, meanwhile the third equation obtains $\boldsymbol{\Gamma}^{-1}\dot{\boldsymbol{\Theta}} = \mathbf{0}$, that is, the parameter vector $\boldsymbol{\Theta}$ is a constant vector, which is just consistent with **Assumption 3.3**.

Consider the differential dynamics of the virtual system (46):

$$\mathcal{M}_2\delta\dot{\boldsymbol{\xi}} = \mathbf{J}_2\delta\boldsymbol{\xi} \tag{47}$$

where $\delta\boldsymbol{\xi} = [\delta\boldsymbol{\xi}_1^T\ \delta\boldsymbol{\xi}_2^T\ \delta\boldsymbol{\xi}_3^T]^T$, $\mathcal{M}_2 = diag(\mathbf{I}_6, \mathbf{M}, \boldsymbol{\Gamma}^{-1})$, and

$$\mathbf{J}_2 = \begin{bmatrix} -\mathbf{K}_p & \mathbf{J}(\boldsymbol{\eta}_2) & \mathbf{0}_{6\times 6} \\ -\mathbf{J}^T(\boldsymbol{\eta}_2) & -(\mathbf{C}(\mathbf{v}) + \mathbf{D}(\mathbf{v}) + \mathbf{K}_D) & -\boldsymbol{\Phi}(\boldsymbol{\eta}_2, \mathbf{v}, \mathbf{v}_r, \dot{\mathbf{v}}_r) \\ \mathbf{0}_{6\times 6} & \boldsymbol{\Phi}^T(\boldsymbol{\eta}_2, \mathbf{v}, \mathbf{v}_r, \dot{\mathbf{v}}_r) & -\mathbf{K}_{\boldsymbol{\Theta}}\boldsymbol{Z}(t) \end{bmatrix} \tag{48}$$

Take $\mathcal{M}_2$ as the metric. The squared length between any two neighboring trajectories under the metric is defined as $V_2 = \delta\boldsymbol{\xi}^T\mathcal{M}_2\delta\boldsymbol{\xi}$, and its time derivative is given as:

$$\dot{V}_2 = 2\delta\boldsymbol{\xi}^T\mathcal{M}_2\delta\dot{\boldsymbol{\xi}} = 2\delta\boldsymbol{\xi}\mathbf{J}_{2,s}\delta\dot{\boldsymbol{\xi}} \tag{49}$$

where $\mathbf{J}_{2,s} = (\mathbf{J}_2 + \mathbf{J}_2^T)/2$ is the symmetric part of $\mathbf{J}_2$:

$$\begin{aligned} \mathbf{J}_{2,s} &= -\begin{bmatrix} \mathbf{K}_p & \mathbf{0}_{6\times 6} & \mathbf{0}_{6\times 6} \\ \mathbf{0}_{6\times 6} & (\mathbf{D}(\mathbf{v}) + \mathbf{K}_D) & \mathbf{0}_{6\times 6} \\ \mathbf{0}_{6\times 6} & \mathbf{0}_{6\times 6} & \mathbf{K}_{\boldsymbol{\Theta}}\boldsymbol{Z}(t) \end{bmatrix} \\ &\leq -\begin{bmatrix} \mathbf{K}_p & \mathbf{0}_{6\times 6} & \mathbf{0}_{6\times 6} \\ \mathbf{0}_{6\times 6} & \mathbf{K}_D & \mathbf{0}_{6\times 6} \\ \mathbf{0}_{6\times 6} & \mathbf{0}_{6\times 6} & \mathbf{K}_{\boldsymbol{\Theta}}\boldsymbol{Z}(t) \end{bmatrix} \end{aligned} \tag{50}$$

Therefore, $\dot{V}_2 \leq -2\lambda_2 V_2$, the virtual system is contracting under the metric $\mathcal{M}_2$ with the contraction rate $\lambda_2 = min\{\lambda_{min}(\mathbf{K}_p), \lambda_{min}(\mathbf{K}_D), \lambda_{\mathbf{Z}}\lambda_{min}(\mathbf{K}_{\boldsymbol{\Theta}})\}/\lambda_{max}(\mathcal{M}_2)$.

According to **Theorem 2.2** and **Lemma 2.3**, this virtual system (46) is contracting if $\lambda_{\mathbf{Z}} > 0$ and semi-contracting if $\lambda_{\mathbf{Z}} \geq 0$. For the former case, $[\boldsymbol{\eta}_d^T\ \mathbf{v}_r^T\ \hat{\boldsymbol{\Theta}}^T]^T \to [\boldsymbol{\eta}^T\ \mathbf{v}^T\ \boldsymbol{\Theta}^T]^T$ exponentially. For the later case, $\delta\boldsymbol{\xi}_1$ and $\delta\boldsymbol{\xi}_2$ tend to zero asymptotically while $\delta\boldsymbol{\xi}_3$ remains

bounded. This gives that $[\boldsymbol{\eta}_d^T \ \mathbf{v}_r^T]^T \to [\boldsymbol{\eta}^T \ \mathbf{v}^T]^T$ asymptotically, and $\hat{\boldsymbol{\Theta}}$ is bounded for all $t \geq 0$.

Definition 4.2. (Persistent Excitation):The regressor $\boldsymbol{\Phi}_f(t) = \boldsymbol{\Phi}_f(\boldsymbol{\eta}_2(t), \mathbf{v}(t)) \in R^{6\times n_{\boldsymbol{\Theta}}}$ is uniformly bounded, it is said to be persistently exciting if there exist $\lambda_{\mathbf{Z}} > 0$ and $T > 0$, such that

$$\int_t^{t+\delta t} e^{-(t-\tau)/\varepsilon_m} \boldsymbol{\Phi}_f^T(\tau)\boldsymbol{\Phi}_f(\tau)d\tau \geq \lambda_{\mathbf{Z}}\mathbf{I}, \forall t \geq T \tag{51}$$

Remark 4.1. Sufficient excitation (SE) and persistent excitation (PE): As pointed out in [55], the SE condition is strictly weaker than the PE condition. A PE regressor always satisfies the SE condition, while the inverse is not true for some combinations of the design parameters.

In most adaptive law, parameter identification, that is, the estimated values of system parameters converges to their real values, will only occur when the PE condition are satisfied. However, as mentioned above, the PE condition is strictly and difficult to meet. The adaptive law proposed in [55] relaxes the strict condition of PE and makes the system identification easier. However, in [55], the adaptive law is only applied to a one DOF manipulator, and only three parameters need to be estimated. In this paper, the effectiveness of the adaptive law is further verified by estimating up to 22 parameters on a more complex AUVs system. In addition, the exponential convergence of the system is analyzed with the framework of contraction theory, which greatly simplifies the design and analysis difficulty of the control system.

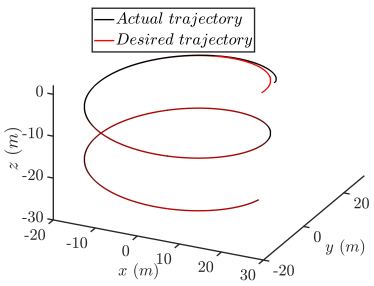

(a)

Fig. 2 Simulation results of ideal controller, the comparison between actual trajectory and desired trajectory

5 Simulation results

Numerical simulations are used in this section to verify the effectiveness of the approaches proposed in this paper. There are two sets of simulations. The first simulation verifies the effectiveness of the ideal controller, while the second verifies the adaptive controller's reliability in the presence of parameter uncertainty and the adaptive law's capacity to achieve parameter identification.

5.1 Simulation of ideal controller

This simulation is used to prove the effectiveness of the ideal controller. The parameters used in this simulation can be found in Appendix [56]. The desired trajectory is a spiral line, which is expressed as:

$$\begin{cases} x_d = 20cos(0.05t) \\ y_d = 20sin(0.05t) \\ z_d = -0.1t \\ \phi_d = 0 \\ \theta_d = atan(\frac{-\dot{z_d}}{\sqrt{\dot{x_d}^2+\dot{y_d}^2}}) \\ \psi_d = atan(\frac{\dot{y_d}}{\dot{x_d}}) \end{cases} \tag{52}$$

The disturbances vector expressed in earth fixed frame is given as $\boldsymbol{\Theta}_c = [-5; -10; 2; 2; 5; 10]$. The control gains of $\mathbf{K}_p$ and $\mathbf{K}_D$ are given as: $\mathbf{K}_p = 0.1\mathbf{I}_6$, $\mathbf{K}_D = 500\mathbf{I}_6$. The initial states of AUV are set as $\boldsymbol{\eta}(0) = [22\ 2\ 2\ 0.1\ 0\ 0.1]^T$ and $\mathbf{v}(0) = \mathbf{0}_{6\times 1}$.

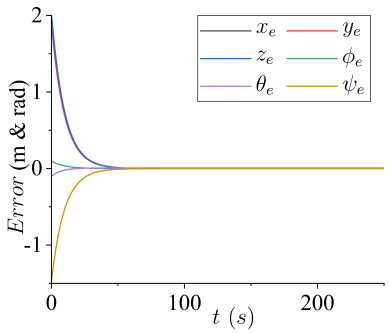

(a)

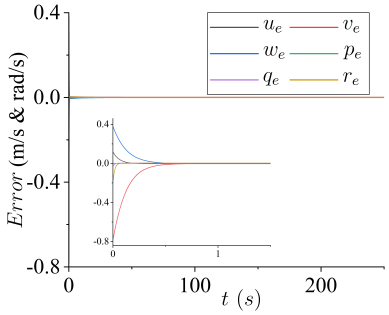

(b)

Fig. 3 Tracking error of ideal controller, (a) position and attitude error, $(\cdot)_e = (\cdot) - (\cdot)_d$; (b) velocity error, $(\cdot)_e = (\cdot) - (\cdot)_r$

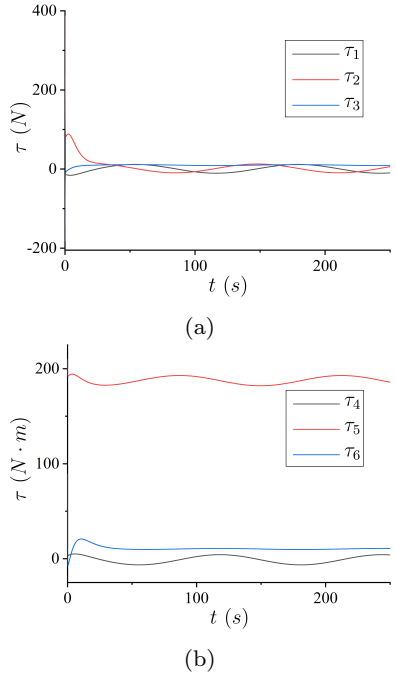

Fig. 4 Control inputs of ideal controller: (a) control forces in surge, sway and heave; (b) control torques in roll, pitch and yaw

As shown in Fig. 2, the ideal controller drives the actual trajectory of the AUV closer to the desired trajectory, and the initial error is quickly eliminated, and then the two trajectories coincide perfectly. Therefore, the control objective is well realized. The position and attitude tracking errors are shown in Fig. 3(a). After about 60s, the AUV has entirely tracked the desired trajectory and the tracking error in each DOF is zero. The errors between the actual velocity and the reference velocity in each DOF are shown in Fig. 3(b). From the local magnification, it can be observed that the velocity error quickly converges to zero in less than one second.

The control inputs of ideal controller are displayed in Fig. 4. Notice that control inputs experience a large fluctuations at the initial tracking stage to eliminate the tracking error, and then stabilized with the gradual reduction of the tracking error. In fact, the control input required at the initial tracking stage is likely to exceed the maximum thrust or torque that the AUVs propeller can provide, resulting in actuator saturation. This problem will be investigated in the future research.

5.2 Simulation of adaptive controller

This part is used to verify the performance of the adaptive controller in the presence of parameter uncertainties and the ability of the adaptive law to realize parameter identification.

The desired trajectory is still a spiral line, which has been given in (52). The disturbances vector is randomly given as $\boldsymbol{\Theta}_c = [-10; -20; 8; 5; 10; 20]$. The simulation parameters are set as follow: $\mathbf{K}_p = 0.2\mathbf{I}_6, \mathbf{K}_D = 100\mathbf{I}_6$, $\boldsymbol{\Gamma} = 100\mathbf{I}_{22}$, $K_{\boldsymbol{\Theta}} = 500\mathbf{I}_{22}$, $\varepsilon_m = 100$ and $\lambda_f = 1$. The initial state of AUV is set as $\boldsymbol{\eta}(0) = [15\ 2\ 2\ 0.1\ 0\ 0.1]^T$ and $\mathbf{v}(0) = \mathbf{0}_{6\times1}$. Assuming that there has no prior knowledge of system parameters, so the initial guess of system parameters is $\hat{\boldsymbol{\Theta}}(0) = \mathbf{0}_{22\times1}$. The tracking results are displayed in Fig. 5, 6 and 7, and the results of parameter estimation are shown in Fig. 8.

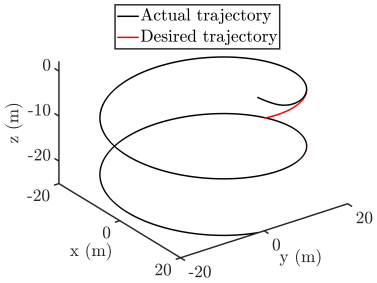

Fig. 5 Simulation results of adaptive, the comparison between actual trajectory and desired trajectory

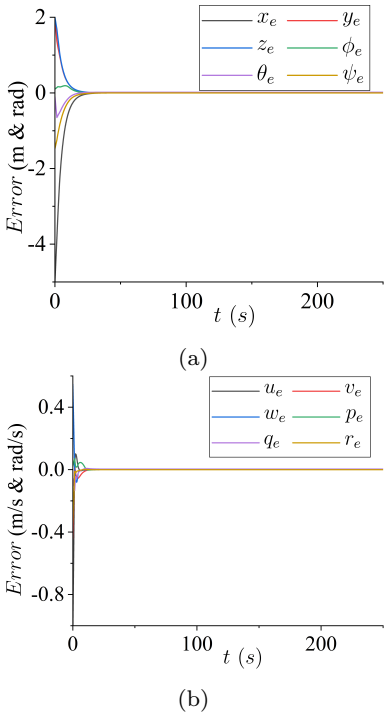

Fig. 6 Tracking errors of adaptive controller, (a) position and attitude error; (b) velocity error

As can be seen from Fig. 5, although the system parameters are unknown, the actual trajectory of AUV

soon coincides with the desired trajectory, and the adaptive controller well realizes the control objective of trajectory tracking. As shown in Fig. 3, the tracking errors of position, attitude and velocity in Fig. 5 quickly converge to zero after a short fluctuation. The control inputs required for adaptive controller are shown in Fig 7. Finally, Fig. 8 shows the results of parameter estimations. It can be seen that for the selected 22 system parameters, their estimated values eventually converge to their real values rather than just remain bounded, and most parameters converge before 30s, and a few parameters converge around 50s. This once again verifies the effectiveness of the adaptive law and provides a method for the parameter identification of AUVs system under specific working conditions.

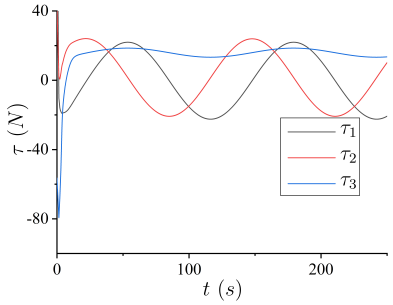

(a)

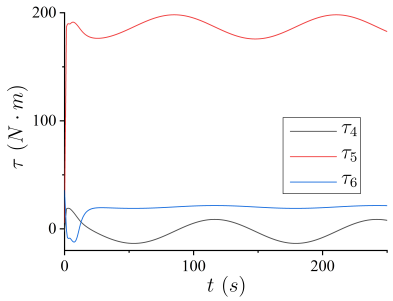

(b)

Fig. 7 Control inuts of adaptive controller, (a) control forces in surge, sway and heave; (b) control torques in roll, pitch and yaw

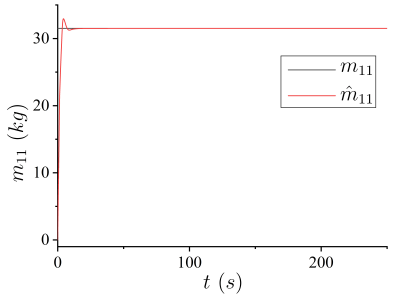

(a)

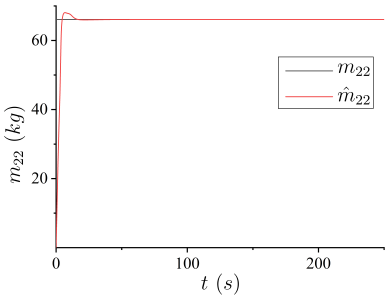

(b)

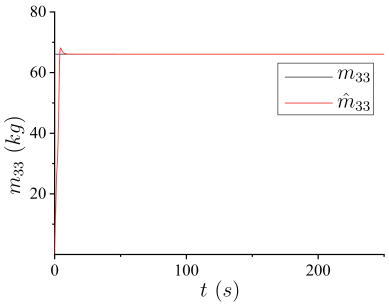

(c)

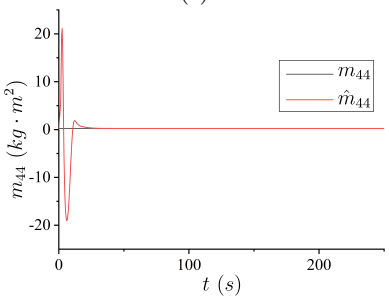

(d)

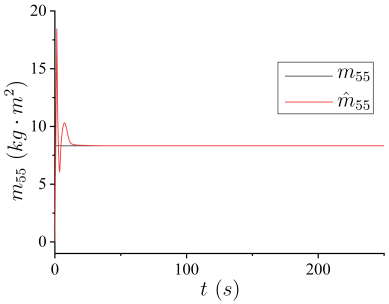

(e)

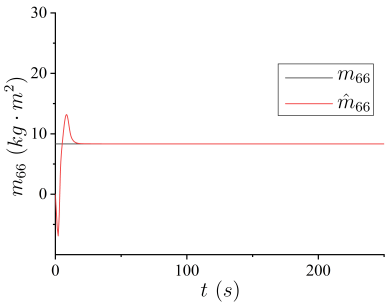

(f)

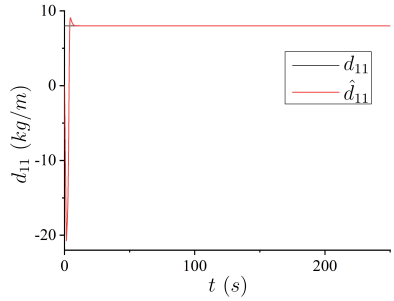
d_{11}
$\hat{d}_{11}$
$d_{11}\ (kg/m)$
$t\ (s)$

(g)

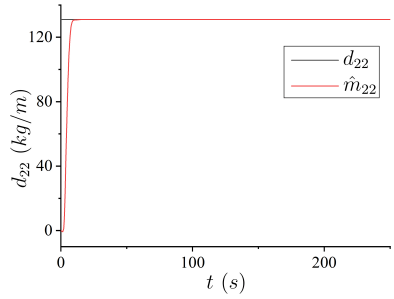
d_{22}
$\hat{m}_{22}$
$d_{22}\ (kg/m)$
$t\ (s)$

(h)

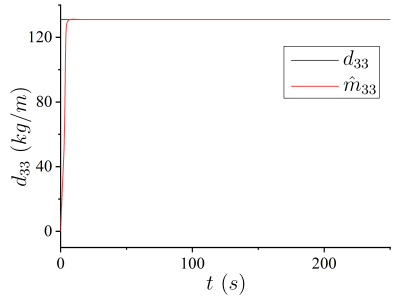
d_{33}
$\hat{m}_{33}$
$d_{33}\ (kg/m)$
$t\ (s)$

(i)

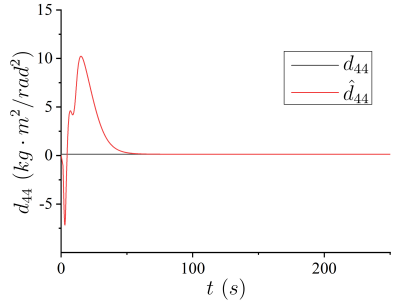
d_{44}
$\hat{d}_{44}$
$d_{44}\ (kg \cdot m^2/rad^2)$
$t\ (s)$

(j)

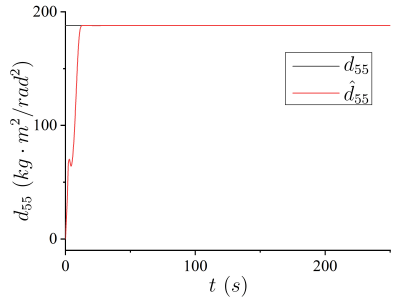
d_{55}
$\hat{d}_{55}$
$d_{55}\ (kg \cdot m^2/rad^2)$
$t\ (s)$

(k)

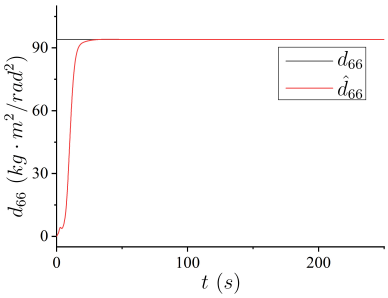
d_{66}
$\hat{d}_{66}$
$d_{66}\ (kg \cdot m^2/rad^2)$
$t\ (s)$

(l)

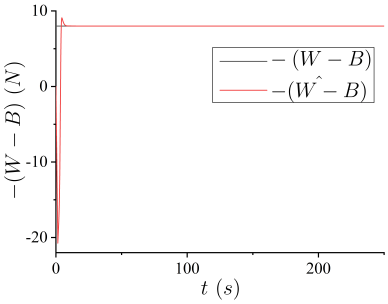
$-(W-B)$
$-(\hat{W}-B)$
$-(W-B)\ (N)$
$t\ (s)$

(m)

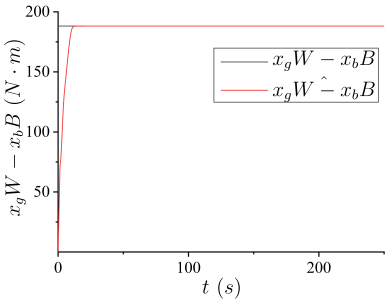
$x_gW - x_bB$
$x_g\hat{W} - x_bB$
$x_gW - x_bB\ (N \cdot m)$
$t\ (s)$

(n)

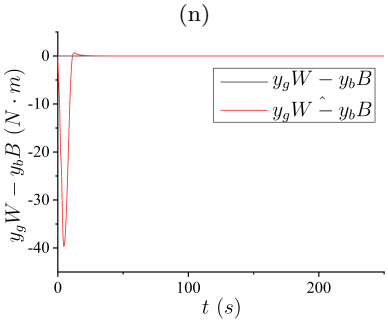
$y_gW - y_bB$
$y_g\hat{W} - y_bB$
$y_gW - y_bB\ (N \cdot m)$
$t\ (s)$

(o)

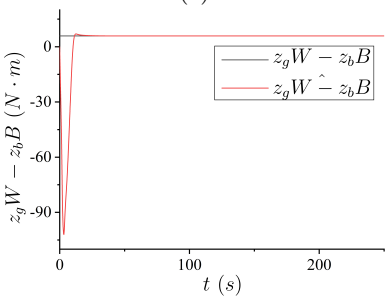
$z_gW - z_bB$
$z_g\hat{W} - z_bB$
$z_gW - z_bB\ (N \cdot m)$
$t\ (s)$

(p)

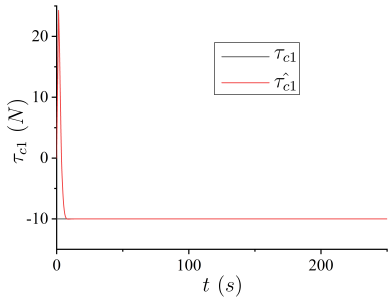

(q)

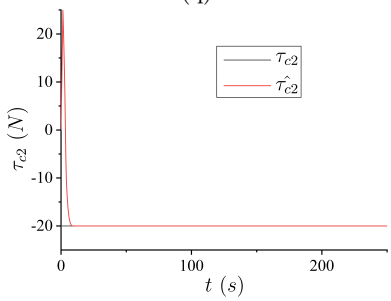

(r)

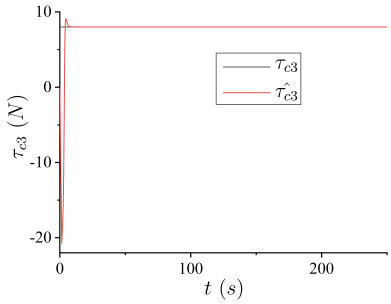

(s)

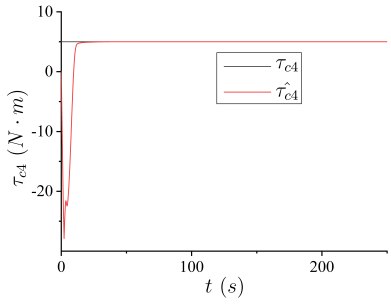

(t)

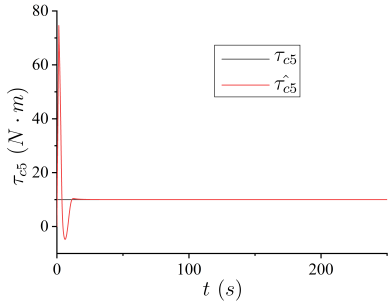

(u)

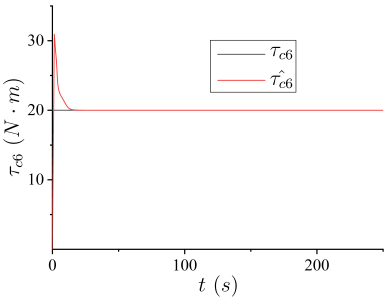

(v)

Fig. 8 Results of parameter estimations by adaptive law

6 Concluding remarks

This paper designs the trajectory tracking controller for a fully-actuated 6-DOF AUV. First, assuming that all system parameters are known, the ideal controller is proposed. Then, an adaptive controller is proposed to deal with parameter uncertainties. Combined with the existing adaptive law, the adaptive controller proposed in this paper not only completes the control objective of trajectory tracking, but also realizes the identification of AUV system parameters without satisfying the PE condition, which provides a new method for obtaining the parameters of AUVs system. The exponential convergence of these controllers is analyzed with the framework of contraction theory. Different from Lyapunov method to study the stability of equilibrium point, contraction theory studies the convergence between any two neighboring trajectories of the system, which is more intuitive for the tracking control problem. In particular, it can be seen that partial contraction, virtual system and modular properties of contraction theory simplify the difficulty of control system design and analysis to a certain extent.

Of course, the research of this paper still has great limitations. Firstly, there are up to 22 parameters that need to be updated online. Although the convergence of these parameters proves the effectiveness of the adaptive law, it also causes a great computational burden. So, it is necessary to establish a more concise AUV model to reduce the computational burden. Then, actuator saturation is ignored in this paper. Finally, from the simulation results of the adaptive controller, it can be seen that the convergence of trajectory and parameters is not synchronous, and the convergence speed between different parameters is also different, which is also noteworthy. Therefore, the next stage of research will focus on the above three points.

Appendix

The parameters of Remus AUV used in this paper [56].

Parameter	Value	Unit
W	300	N
B	308	N
m	30.58	kg
I_x	0.177	$kg \cdot m^2$
I_y	3.45	$kg \cdot m^2$
I_z	3.45	$kg \cdot m^2$
x_g	0	m
y_g	0	m
z_g	0.00196	m
x_b	-0.0611	m
y_b	0	m
z_b	0	m
$X_{\dot{u}}$	-0.93	kg
$Y_{\dot{v}}$	-35.5	kg
$Z_{\dot{w}}$	-35.5	kg
$K_{\dot{p}}$	-0.0704	$kg \cdot m^2$
$M_{\dot{q}}$	-4.88	$kg \cdot m^2$
$N_{\dot{r}}$	-4.88	$kg \cdot m^2$
$X_{\|u\|u}$	-1.62	kg/m
$Y_{\|v\|v}$	-131	kg/m
$Z_{\|w\|w}$	-131	kg/m
$K_{\|p\|p}$	-0.13	$kg \cdot m^2/rad^2$
$M_{\|q\|q}$	-188	$kg \cdot m^2/rad^2$
$N_{\|r\|r}$	-94	$kg \cdot m^2/rad^2$

References

1. Yuh, J.: Design and control of autonomous underwater robots: a survey. Autonoumous Robots. **8**, 7-24 (2000)
2. Nicholson, J.W., Healey, A.J.: The present state of autonomous underwater vehicle (AUV) applications and technologies. Marine Technology Society Journal. **42**(1), 44-51 (2008)
3. Khodayari, M.H., Balochian, S.: Modeling and control of autonomous underwater vehicle (AUV) in heading and depth attitude via self-adaptive fuzzy PID controller. Journal of Marine Science and Technology. **20**(3), 559-578 (2015)
4. Koh, T.H., Lau, M.W.S., Seet, G., Low, E.: A Control Module Scheme for an Underactuated Underwater Robotic Vehicle. Journal of Intelligent and Robotic Systems. **46**(1), 43-58 (2006)
5. Gharesi, N., Ebrahimi, Z., Forouzandeh, A., Arefi, M.M.: Extended state observer-based backstepping control for depth tracking of the underactuated AUV. In: 5th International Conference on Control, Instrumentation, and Automation (ICCIA), pp. 354-358 (2017)
6. Wang, J., Wang, C., Wei, Y., Zhang, C.: Three-Dimensional Path Following of an Underactuated AUV Based on Neuro-Adaptive Command Filtered Backstepping Control. IEEE Access. **6**, 74355-74365 (2018)
7. Fossen, T.I., Fjellstad, O.-E.: Robust adaptive control of underwater vehicles: A comparative study. Modeling, Identification and Control: A Norwegian Research Bulletin. **17**(1), 47-61 (1996)
8. Antonelli, G., Chiaverini, S., Sarkar, N., West, M.: Adaptive control of an autonomous underwater vehicle: experimental results on ODIN. IEEE Transactions on Control Systems Technology. **9**(5), 756-765 (2001)
9. Antonelli, G., Caccavale, F., Chiaverini, S., Fusco, G.: A novel adaptive control law for underwater vehicles. IEEE Transactions on Control Systems Technology. **11**(2), 221-232 (2003)
10. Yuh, J., Nie, J.: Application of non-regressor-based adaptive control to underwater robots: experiment. Computers & Electrical Engineering. **26**(2), 169-179 (2000)
11. Healey, A.J., Lienard, D.: Multivariable sliding mode control for autonomous diving and steering of unmanned underwater vehicles. IEEE journal of Oceanic Engineering. **18**(3), 327-339 (1993)
12. Elmokadem, T., Zribi, M., Youcef-Toumi, K.: Trajectory tracking sliding mode control of underactuated AUVs. Nonlinear Dynamics. **84**(2), 1079-1091 (2015)
13. Qiao, L., Zhang, W.: Trajectory Tracking Control of AUVs via Adaptive Fast Nonsingular Integral Terminal Sliding Mode Control. IEEE Transactions on Industrial Informatics. **16**(2), 1248-1258 (2020)
14. Shen, C., Shi, Y., Buckham, B.: Trajectory Tracking Control of an Autonomous Underwater Vehicle Using Lyapunov-Based Model Predictive Control. IEEE Transactions on Industrial Electronics. **65**(7), 5796-5805 (2018)
15. Shen, C., Shi, Y., Buckham, B.: Path-Following Control of an AUV: A Multiobjective Model Predictive Control Approach. IEEE Transactions on Control Systems Technology. **27**(3), 1334-1342 (2019)
16. Miao, J., Wang, S., Zhao, Z., Li, Y., Tomovic, M.M.: Spatial curvilinear path following control of underactuated AUV with multiple uncertainties. ISA transactions. **67**, 107-130 (2017)
17. Huang, Z., Liu, Y., Zheng, H., Wang, S., Ma, J., Liu, Y.: A self-searching optimal ADRC for the pitch angle control of an underwater thermal glider in the vertical plane motion. Ocean Engineering. **159**, 98-111 (2018)
18. Hsu, H.H., Wu, Y.C.: The hydrodynamic coefficients for an oscillating rectangular structure on a free surface with sidewall. Ocean Engineering. **24**(2), 177-199 (1997)
19. Ramos, J., Soares, C.G.: On the assessment of hydrodynamic coefficients of cylinders in heaving. Ocean engineering. **24**(8), 743-763 (1997)
20. Shahbazi, M., Mansourzadeh, S., Pishevar, A.R.: Hydrodynamic analysis of autonomous underwater vehicle (AUV) flow through boundary element method and computing added-mass coefficients. International Journal of Artifical Intelligence and Mechatronics. **3**, 212-217 (2015)
21. Jagadeesh, P., Murali, K., Idichandy, V.G.: Experimental investigation of hydrodynamic force coefficients over AUV hull form. Ocean Engineering. **36**(1), 113-118 (2009)
22. Avila, J.P.J., Adamowski, J.C.: Experimental evaluation of the hydrodynamic coefficients of a ROV through Morison's equation. Ocean Engineering. **38**(17-18), 2162-2170 (2011)
23. Zhang, H., Xu, Y.-r., Cai, H.-p.: Using CFD software to calculate hydrodynamic coefficients. Journal of Marine Science and Application. **9**(2), 149-155 (2010)
24. Pan, Y.-c., Zhang, H.-x., Zhou, Q.-d.: Numerical Prediction of Submarine Hydrodynamic Coefficients using CFD Simulation. Journal of Hydrodynamics. **24**(6), 840-847 (2012)
25. Gao, T., Wang, Y., Pang, Y., Chen, Q., Tang, Y.: A time-efficient CFD approach for hydrodynamic coefficient determination and model simplification of submarine. Ocean Engineering. **154**, 16-26 (2018)
26. Astrom, K.J., Kumar, P.R.: Control: A perspective. Automatic. **50**(1), 3-43 (2014)

27. Do, K.D., Pan, J., Jiang, Z.P.: Robust and adaptive path following for underactuated autonomous underwater vehicles. Ocean Engineering. **31**(16), 1967-1997 (2004)
28. Sahu, B.K., Subudhi, B.: Adaptive Tracking Control of an Autonomous Underwater Vehicle. International Journal of Automation and Computing. **11**(3), 299-307 (2015)
29. Sun, Y.C., Cheah, C.C.: Adaptive control schemes for autonomous underwater vehicle. Robotica. **27**(1), 119-129 (2009)
30. Li, J., Du, J., Zhu, G., Lewis, F.L.: Simple adaptive trajectory tracking control of underactuated autonomous underwater vehicles under LOS range and angle constraints. IET Control Theory & Applications. **14**(2), 283-290 (2020)
31. Rezazadegan, F., Shojaei, K., Sheikholeslam, F., Chatraei, A.: A novel approach to 6-DOF adaptive trajectory tracking control of an AUV in the presence of parameter uncertainties. Ocean Engineering. **107**, 246-258 (2015)
32. Zhu, C., Huang, B., Zhou, B., Su, Y., Zhang, E.: Adaptive model-parameter-free fault-tolerant trajectory tracking control for autonomous underwater vehicles. ISA transactions. **114**, 57-71 (2021)
33. Lohmiller, W., Slotine, J.J.E.: On contraction analysis for non-linear systems. Automatica. **34**(6), 683-696 (1998)
34. Jouffroy, J., Slotine, J.J.E.: Methodological remarks on contraction theory. In: 43rd IEEE Conference on Decision and Control (CDC), **3**, 2537-2543 (2004)
35. Forni, F., Sepulchre, R.: A Differential Lyapunov Framework for Contraction Analysis. IEEE Transactions on Automatic Control. **59**(3), 614-628 (2014)
36. Tsukamoto, H., Chung, S.-J., Slotine, J.-J.E.: Contraction theory for nonlinear stability analysis and learning-based control: A tutorial overview. Annual Reviews in Control. **52**, 135-169 (2021)
37. Wang, W., Slotine, J.J.: On partial contraction analysis for coupled nonlinear oscillators. Biological cybernetics. **92**(1), 38-53 (2005)
38. Lohmiller, W., Slotine, J.J.E.: Control system design for mechanical systems using contraction theory. IEEE Transactions on Automatic Control. **45**(5), 984-989 (2000)
39. Jouffroy, J., Opderbecke, J.: Underwater Vehicle Navigation Using Diffusion-Based Trajectory Observers. IEEE Journal of Oceanic Engineering. **32**(2), 313-326 (2007)
40. Russo, G., Di Bernardo, M., Sontag, E.D.: Stability of networked systems: A multi-scale approach using contraction. In: 49th IEEE Conference on Decision and Control (CDC), 6559-6564 (2010)
41. Del Vecchio, D., Slotine, J.E.: A Contraction Theory Approach to Singularly Perturbed Systems. IEEE Transactions on Automatic Control. **58**(3), 752-757 (2013)
42. Chavez-Moreno, R., Tang, Y., Hernandez, J.-C., Ji, H.: Contracting Angular Velocity Observer For Small Satellites. IEEE Transactions on Aerospace and Electronic Systems. **54**(6), 2762-2775 (2018)
43. Singh, S., Majumdar, A., Slotine, J.J., Pavone, M.: Robust online motion planning via contraction theory and convex optimization. In: IEEE International Conference on Robotics and Automation (ICRA), 5883-5890 (2017)
44. Tsukamoto H., Chung, S.J.: Robust controller design for stochastic nonlinear systems via convex optimization. IEEE Transactions on Automatic Control. **66**(10), 4731-4746 (2020)
45. Jouffroy, J.: A relaxed criterion for contraction theory: Application to an underwater vehicle observer. In: European Control Conference (ECC), 2999-3004 (2003)
46. Jouffroy, J., Fossen, T.I.: On the combination of nonlinear contracting observers and UGES controllers for output feedback. In: 43rd IEEE Conference on Decision and Control (CDC), **5**, 4933-4939 (2004)
47. Mohamed, M., Swaroop, S.: Incremental input to state stability of underwater vehicle. IFAC-PapersOnLine. **49**(1), 41-46 (2016)
48. Mohamed, M., Su, R.: Contraction based tracking control of autonomous underwater vehicle. IFAC-PapersOnLine. **50**(1), 2665-2670 (2017)
49. Reyes-Báez R, van der Schaft A, Jayawardhana B, et al: Tracking control of marine craft in the port-Hamiltonian framework: A virtual differential passivity approach. In: 2019 18th European Control Conference (ECC), 1636-1641 (2019)
50. Reyes Báez, R.: Virtual contraction and passivity based control of nonlinear mechanical systems: trajectory tracking and group coordination. University of Groningen (2019)
51. Torsetnes, G., Jouffroy, J., Fossen, T.I.: Nonlinear dynamic positioning of ships with gain-scheduled wave filtering. In: 43rd IEEE Conference on Decision and Control (CDC), **5**, 5340-5347 (2004)
52. Zhang, Y.F., Liu, C.D.: High-Gain Disturbance Observer-Based Backstepping Control for Dynamic Positioning Ships Using Contraction Theory. In: 39th Chinese Control Conference (CCC), 282-287 (2020)
53. Society of Naval Architects and Marine Engineers (SNAME): Nomenclature for Treating the Motion of a Submerged Body through a Fluid. Technical Research Bulletin No. 1-5 (1950)
54. Fossen, T.I.: Handbook of marine craft hydrodynamics and motion control. John Wiley & Son. (2011)
55. Tang, Y., Arteaga, M.A.: Adaptive control of robot manipulators based on passivity. IEEE Transactions on Automatic Control. **39**(9), 1871-1875 (1994)
56. Prestero, T.T.J.: Verification of a six-degree of freedom simulation model for the REMUS autonomous underwater vehicle. Massachusetts institute of technology (2001)

Statements & Declarations

Acknowledgements

The authors would like to thank the financial support by the Foundation of Pre-research on Military Equipment of the Chinese People's Liberation Army (No. 6140241010103; JZX7Y20190252032901).

Competing Interests

The authors declare that they have no known competing financial interests or personal relationships that could have appeared to influence the work reported in this paper.

Author Contributions

Caipeng. Ma: Investigation, Conceptualization, Methodology, Formula analysis, Data curation, Writing-original draft, Writing – review & editing, Validation, Visualization. **Yu Tang:** Conceptualization, Methodology, Validation, Review & Editing. **Jiaxi Wang:** Formula anal-

ysis, Post-processing, Data curation, Review & Editing. **Jiajie Yan:** Post-processing, Data curation, Review & Editing. **Yuchen Liao:** Post-processing, Review & Editing, Visualization. **Dapeng Jiang:** Review & Editing, Conceptualization, Resources, Supervision, Funding acquisition, Project administration.

Data Availability

The datasets generated during and/or analysed during the current study are available from the corresponding author on reasonable request.